Journal of the European Ceramic Society **19** (1999) 2781–2787

PII: S0955-2219(99)00072-2
0955-2219/99/$ - see front matter

Thermodynamics of the Al–C–O System and Properties of SiC–AlN–Al_2OC Composites

J.-M. Lihrmann,[a]* J. Tirlocq,[b] P. Descamps[b] and F. Cambier[b]

[a]LIMHP, UPR CNRS 1311, Avenue J.-B. Clément, 93430 Villetaneuse, France
[b]CRIBC, 4 Avenue Gouverneur Cornez, 7000 Mons, Belgium

(Received 15 August 1998; accepted 13 March 1999)

Abstract

Based on a recent thermodynamic evaluation of the Al–C–O system, the standard Gibbs free energies of formation of both aluminium oxycarbides Al_4O_4C *and* Al_2OC *are given, and a classical stability diagram is shown at 2100 K. Because* Al_2OC *is unstable below 1715 °C, the stable würtzite compound* $2AlN.Al_2OC$ *has been preferred, and formed in-situ as the second phase in SiC-based composites. Starting with commercial powders of α-SiC, AlN,* Al_2O_3 *and* Al_4C_3*, dense materials are obtained by pressureless sintering (up to 2020 °C) or hot-pressing (up to 1950 °C), owing to the liquid phase from the* Al_2O_3*–*Al_4C_3 *system. The existence of a miscibility gap is shown, and the microstructures are fine grained and equiaxed. Compared with SiC–*Al_2OC *alloys, the hot-pressed materials with 90 wt% SiC exhibit slightly higher mechanical properties and a good retention nearly up to 1500 °C. © 1999 Elsevier Science Ltd. All rights reserved*

Résumé

A partir d'une évaluation thermodynamique récente du système Al–C–O, les enthalpies libres molaires de formation standard des oxycarbures d'aluminium Al_4O_4C *et* Al_2OC *sont données, et un diagramme de stabilité classique est présenté à 2100 K. En raison de l'instabilité de* Al_2OC *en-dessous de 1715 °C, le composé würtzite stable* $2AlN.Al_2OC$ *a été préféré, et est formé in-situ comme seconde phase dans des composites à base de SiC. A partir de poudres commerciales de α-SiC, AlN,* Al_2O_3 *et* Al_4C_3*, des matériaux denses sont obtenus par frittage naturel (jusqu'à 2020 °C) ou par pressage à chaud (jusqu'à 1950 °C) grâce à la phase liquide du système* Al_2O_3*–*Al_4C_3*. On observe l'existence d'une lacune de miscibilité, et les microstructures sont à grains fins et équiaxes. Comparables aux alliages SiC–*Al_2OC*, les composites pressés à chaud contenant 90% de SiC en poids présentent cependant de meilleures propriétés mécaniques et leur maintien pratiquement jusqu'à 1500 °C. © 1999 Elsevier Science Ltd. All rights reserved*

Keywords: Al_2OC, sintering, composites, mechanical properties, SiC.

1 Introduction

Silicon carbide (SiC) is one of the promising ceramic candidates for high temperature structural applications because of its excellent mechanical and abrasive properties, its high thermal conductivity and corrosion resistance, its low density and thermal expansion coefficient, but the covalent nature of its atomic bonding makes it difficult to densify. SiC is converted into more or less dense parts by infiltration of porous preforms or by sintering. While fully dense parts are obtained by hot-pressing, usually at temperatures between 1900 and 2000 °C and pressures up to 50 MPa, highly dense parts (i.e. $>95\%$ of theoretical density) may be obtained by pressureless sintering. In solid state sintering, small amounts of additives (e.g. 0.5–2 wt% boron and carbon) are needed to densify either β-SiC[1] or α-SiC.[2] The requested temperatures exceed 2000 °C and may be responsible for phase transformations ($\beta \rightarrow \alpha$) or exaggerated grain growth, in which case the elongated grains can act as microstructural defects and decrease the modulus of rupture.

An interesting feature is brought by liquid phase sintering, where added oxides are selected to create a liquid phase at lower temperatures (1850–1900 °C), thereby reducing densification times and exaggerated grain growth. The most frequent oxide additives for SiC are rare-earth oxides, typically

---

* To whom correspondence should be addressed.

Y_2O_3, often combined with Al_2O_3 and AlN under various forms of precursors,[3] in order to take advantage of one of the eutectics of the system Al_2O_3–Y_2O_3. Following the same strategy the system Al_2O_3–Al_4C_3 has been used in combination with SiC, to fabricate SiC–Al_2OC alloys.[4,5] The present paper investigates the influence of the addition of aluminum nitride on the processing and properties of SiC–Al_2OC–AlN composites. The motivation to add aluminum nitride to aluminum oxide and aluminum carbide was suggested by recent experimental observations[6,7] and modelling[8,9] which indicated that (i) pure Al_2OC is stable only above 1715 °C and (ii) dissolution of AlN in Al_2OC forms a würtzite compound of increased stability. From the compositions selected here it is shown that two-phase composites are obtained, made of SiC and an Al_2OC.AlN solid solution which is formed *in-situ* in amounts between 5 and 90 wt%. Before describing the results, the thermodynamics of the Al–C–O system are briefly recalled.

2 Experimental

Commercial powders of SiC (Silicon carbide A10, α variety, Hermann C. Starck GmbH, Goslar, Germany), AlN (Aluminium Nitride Grade B, Hermann C. Starck GmbH, Goslar, Germany), Al_2O_3 (Alumina Grade A16SG, Alcoa Industrial Chemicals, Bauxite, AR) and Al_4C_3 (Aluminium Carbide Grade D, Hermann C. Starck GmbH, Goslar, Germany) were used to prepare the compositions 1–10 of Fig. 1. Weighing and mixing were done under argon in order to limit the oxidation of AlN and Al_4C_3 powders. Slurries with 40 wt% of dry powder in isopropanol were milled for 16 h in sealed polyethylene vessels using a vibratory mill, and dried under vacuum. The powders were then ground, sieved at 180 μm and stored in argon. Compositions 1–10 were densified by hot-pressing at 30 MPa and 1950 °C, under nitrogen or in vacuum; the heating rate was 5 °C min^{-1}, with no soaking time. For pressureless sintering, powders (90 wt% SiC) were shaped into disks of diameter 50 mm without binder (uniaxial compaction at 30 MPa followed by cold isostatic pressing at 180 MPa). Those disks were embedded in a powder bed inside a closed graphite crucible sealed with a threaded graphite cap using graphite foil. Heating was done in a graphite furnace under argon with respective heating rates of 10 °C min^{-1} up to 1500 °C and 5 °C min^{-1} up to 2020 °C, followed by a 50 min soaking period.

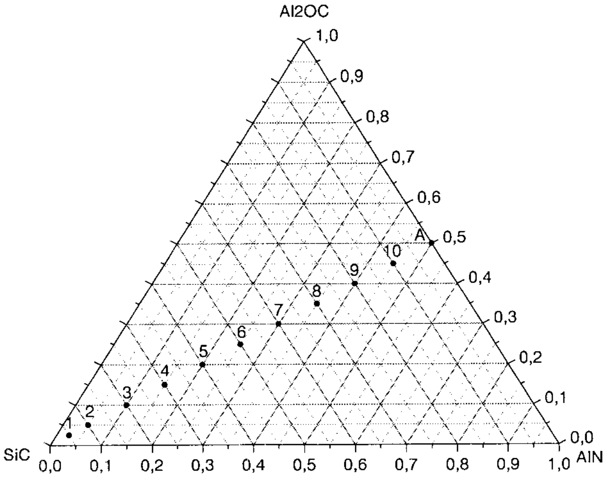

Fig. 1. Compositions investigated, in wt%. Compound A is (2AlN).Al_2OC.

After cooling, the samples were ground for X-Ray analysis. Densities and open porosities were measured using Archimede's method; the microstructure was characterised by optical and electron microscopy.

The following mechanical properties were measured: Vickers hardness, 3-point bending strength, Young's modulus, fracture toughness and creep resistance. Vickers hardness was measured by applying for 20 s, a 500 g load with a diamond indenter on polished surfaces. Flexural strength was measured up to 1500 °C, on bend bars having dimensions 40×4×3 mm. The stress–strain curves of the 3-point bend tests provided the values of both flexural strength (σ_f) and Young's modulus (E); K_{IC} was measured using the single-edge V-notched beam (SEVNB) method. Compared with the SENB technique, it uses bars having a V shaped notch with a sharp tip radius,[10] therefore avoiding the problem of K_c overestimation.[11] Creep tests were performed on bend bars with the same dimensions as previously, under 103 MPa in argon, at 1400 and 1500 °C. The creep rate, $\dot{\varepsilon}$, was calculated using Hollenberg's equation:[12] $\dot{\varepsilon} = 2h(n+2)\dot{\delta}/L^2$, where h is the samples' thickness, L the span and $\dot{\delta}$ the deflection rate of the samples' upper surface; n was assumed equal to 1 (Newtonian creep).

3 Results and Discussion

3.1 Thermodynamics of the Al–C–O system

The Al_2O_3–Al_4C_3 phase diagram has been recently calculated by Qiu and Metselaar,[8] in excellent agreement with experimental observations. Complementary data obtained from their evaluation are listed in Table 1. It follows from Table 1 that the reaction $Al_4O_4C + Al_4C_3 = 4Al_2OC$, for which $\Delta_rG°(J) = -45100 + 696.9472T - 88.8TLnT$, is thermodynamically impossible at all temperatures below 1983 K (1710 °C), in consistency with the observed value[6] of 1715 °C.

Table 1. Gibbs free energies of formation of solid components in the Al–C–O system, in S.I. units (J, mole, K)[a]

Al_4C_3

$1000 \leq T \leq 2100$

$\Delta_f G^\circ = -209944{\cdot}693 - 282{\cdot}185012\ T + 51{\cdot}158268\ TLnT - 153{\cdot}16705 \times 10^{-4}\ T^2 + 3{\cdot}633 \times 10^{-10}\ T^3 - 9551482/T + 7{\cdot}929 \times 10^8/T^2 - 3{\cdot}6 \times 10^{10}/T^3$

Al_2O_3

$1000 \leq T \leq 1500$

$\Delta_f G^\circ = -1703587{\cdot}779 + 362{\cdot}016573\ T - 2{\cdot}320216\ TLnT - 54{\cdot}38306 \times 10^{-4}\ T^2 + 2581{\cdot}89 \times 10^{-10}\ T^3 + 1331985/T$

$1500 \leq T \leq 2100$

$\Delta_f G^\circ = -1750864{\cdot}909 + 660{\cdot}6148\ T - 42{\cdot}120216\ TLnT + 88{\cdot}78444 \times 10^{-4}\ T^2 - 6497{\cdot}45 \times 10^{-10}\ T^3 + 11577935/T$

Al_4O_4C

$1000 \leq T \leq 1500$

$\Delta_f G^\circ = -2352531{\cdot}936 + 388{\cdot}627099\ T + 13{\cdot}959135\ TLnT - 123{\cdot}56643 \times 10^{-4}\ T^2 + 3443{\cdot}7 \times 10^{-10}\ T^3 - 1407847{\cdot}333/T + 2{\cdot}643 \times 10^8/T^2 - 1{\cdot}2 \times 10^{10}/T^3$

$1500 \leq T \leq 2100$

$\Delta_f G^\circ = -2415568{\cdot}109 + 786{\cdot}758068\ T - 39{\cdot}107532\ TLnT + 67{\cdot}32357 \times 10^{-4}\ T^2 - 8662{\cdot}056 \times 10^{-10}\ T^3 + 12253419{\cdot}34/T + 2{\cdot}643 \times 10^8/T^2 - 1{\cdot}2 \times 10^{10}/T^3$

Al_2OC

$1000 \leq T \leq 1500$

$\Delta_f G^\circ = -651894{\cdot}1573 + 200{\cdot}8473217\ T - 5{\cdot}920649\ TLnT - 69{\cdot}18337 \times 10^{-4}\ T^2 + 861{\cdot}841 \times 10^{-10}\ T^3 - 2739832{\cdot}333/T + 2{\cdot}643 \times 10^8/T^2 - 1{\cdot}2 \times 10^{10}/T^3$

$1500 \leq T \leq 2100$

$\Delta_f G^\circ = -667653{\cdot}2006 + 300{\cdot}380064\ T - 19{\cdot}187316\ TLnT - 21{\cdot}46087 \times 10^{-4}\ T^2 - 2164{\cdot}606 \times 10^{-10}\ T^3 + 675484{\cdot}334/T + 2{\cdot}643 \times 10^8/T^2 - 1{\cdot}2 \times 10^{10}/T^3$

[a] Among the previously existing data, the expression[13] $\Delta_f G^\circ$ (Al_4O_4C) = $-2333307 + 463{\cdot}214$ T (J.mol^{-1}) is within 0·6% error with the above description in the range 1000–2100 K.

This temperature becomes much lower in the presence of aluminum nitride, due to the formation of an Al_2OC.AlN würtzite solid solution. Although phase separation occurs upon annealing, it does so into stable Al_2OC-rich precipitates, as was observed[14] after a 61%AlN–39% Al_2OC solid solution was exposed at 1600 °C for 500 h. In comparison, pure Al_2OC would decompose into Al_4O_4C and Al_4C_3 after a 15 min exposure at 1700 °C,[6] and the sample would be soon entirely damaged due to the large sensitivity to moisture of aluminum carbide.

The high temperature volatilisation of the solid species of the Al–C–O system into Al(g), Al_2O (g), AlO(g) or AlO_2(g), is responsible for important weight losses and prevents densification by pressureless sintering if special care is not taken, as observed for Al_2OC in the present work and previously reported by other authors.[4,5] The stability diagram of the Al–C–O system at 2100 K is represented in Fig. 2, where according to the usual practice only the predominating gas species is mentioned. The thermodynamic descriptions used for this diagram were taken from Table 1 for the solid components and from Janaf Tables[15] for the gas species. It clearly appears that the stability field of both oxycarbides is narrow, between carbon monoxide pressures of 0·1306 and 0·1644 atm for Al_2OC and between CO pressures of 0·1644 and 0·2361 atm for Al_4O_4C.

3.2 Characterisation of the composites

X-ray analysis of both hot-pressed and pressureless sintered samples revealed α-SiC and a second phase. No trace of Al_4O_4C, Al_4C_3 or pure Al_2OC was detected. The major polytype of α-SiC was 6H, but minor amounts of 4H and 15R were also present. The interplanar spacings of the second phase were nearly independent of its amount in the compositions, and intermediate between those of AlN and Al_2OC, as can be seen in Table 2 for compositions 1–6. Based on previous investigations of the AlN–Al_2OC pseudo-binary system, which identified continuous AlN–Al_2OC (2H) solid solutions in the respective ranges 0–44 mol% Al_2OC at 1880 °C[14] and 0–40 mol% at 1980 °C,[6] the second phase of the present study, with an Al_2OC content of 33 mol%, clearly belongs to this solid solution. Assuming there was no change in composition during heating, it will be referred to as 2AlN.Al_2OC. The constant presence of this phase regardless of the composition, is best explained by the occurrence of a miscibility gap in the pseudo-binary system SiC–2AlN.Al_2OC, between an SiC-rich phase and a AlN.Al_2OC-rich phase. In spite of the similarity between the crystal structures[16] of SiC and 2AlN.Al_2OC, a continuous single phase solid solution is thus not formed at about 2000 °C in the pseudo-binary system SiC–AlN.Al_2OC, as it is also observed in the binary systems SiC–Al_2OC[4,5] and SiC–AlN.[17]

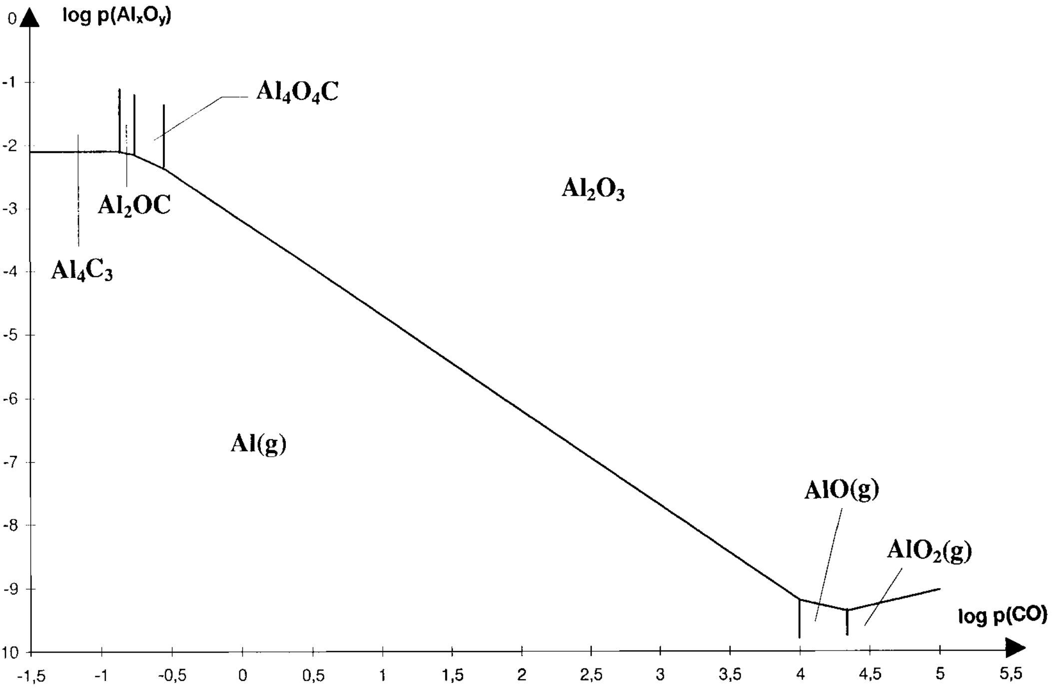

Fig. 2. Stability diagram of the Al–C–O system at 2100 K (pressures expressed in atm).

Table 2. Interplanar spacings of the second phase in the composites

wt% solid solution in composite	*Spacings (A) between planes (hkl)*				
	(100)	*(101)*	*(102)*	*(110)*	*(103)*
5	2·730	2·391	1·841	1·562	1·422
10	2·720	3·391	1·842	1·564	1·422
20	2·724	2·393	1·845	1·568	1·423
30	2·724	2·393	1·845	1·569	1·423
40	2·721	2·392	1·845	1·568	1·423
50	2·721	2·392	1·845	1·568	1·423
AlN[6]	2·700	2·372	1·829	1·557	1·414
Al_2OC[24]	2·75	2·42	1·87	1·58	1·45

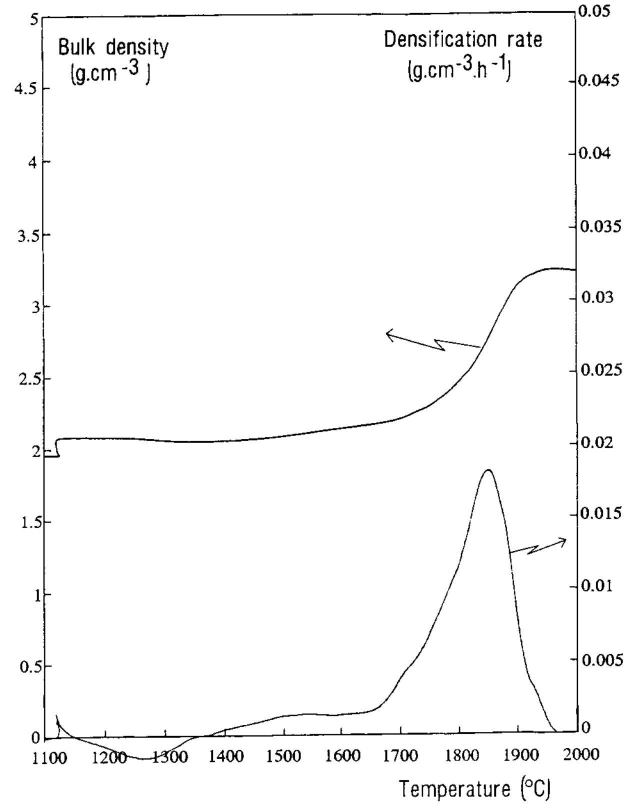

Fig. 3. Typical densification curve and kinetics of hot-pressed materials.

Based on the rule of mixtures with values of 3·255 for AlN[18] and 3·095 for Al_2OC,[19] the theoretical density of $2AlN.Al_2OC$ is 3·173. The theoretical density of the different mixtures was calculated in the same way, using 3·217 for SiC.[20] In these conditions, the hot-pressed samples of compositions 1–7 have relative densities in excess of 99·7%. A typical densification curve of hot-pressed materials is shown on Fig. 3 along with the densification kinetics.[21] Regardless of the composition, sintering essentially occurs between 1800 and 1900°C, the maximum density being reached slightly above 1900°C with a maximum densification rate at about 1850°C. These temperatures coincide with the formation of a liquid phase at 1840°C in the system Al_2O_3–Al_4C_3, as was also noticed for the formation of Al_2OC[7] and for the densification of SiC–Al_2O_3–Al_4C_3 mixtures.[4] In the case of pressureless sintering, the final densities vary between 86 and 96% depending on the soaking temperature,[21] as shown in Fig. 4 for the composite with 90 wt% SiC. Also shown in this figure are two densification curves from Ref. 5, relative to SiC–Al_2OC materials sintered, respectively, in Ar and N_2 with a 5 min hold. The densification of the present

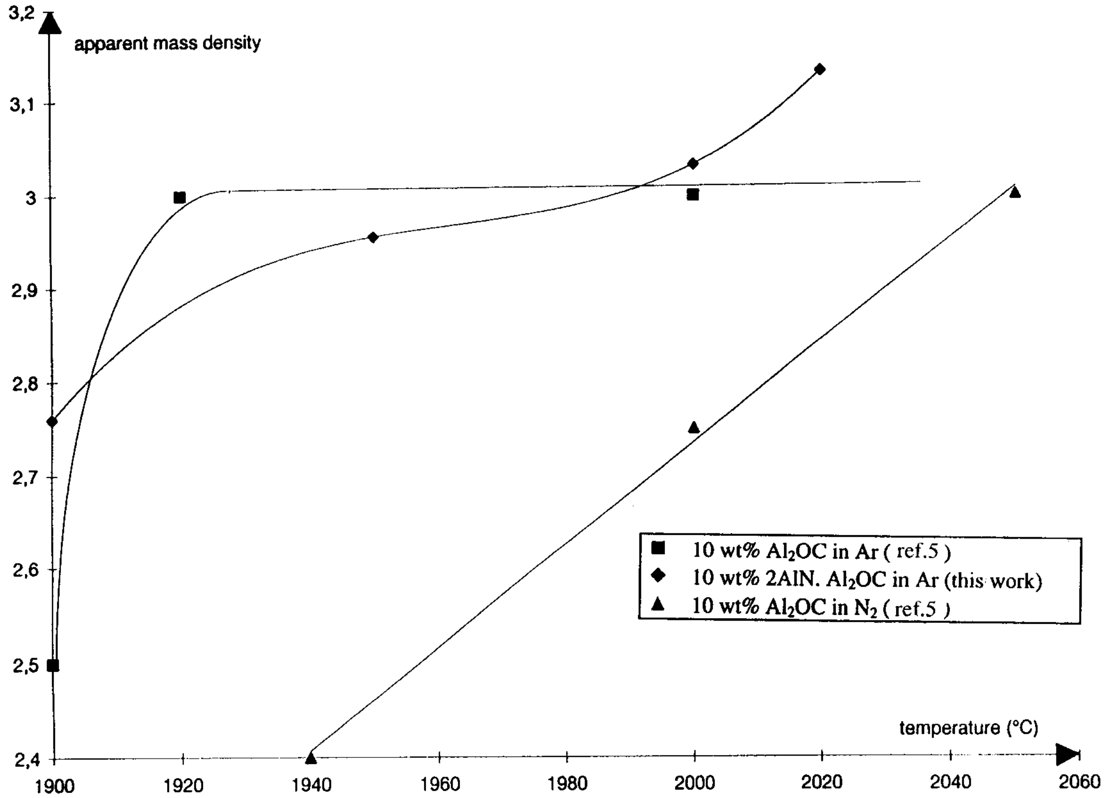

Fig. 4. Densification curves of some composites with 90 wt% SiC, by pressureless sintering in various environments.

composites is evidently more gradual than that of SiC–Al_2OC alloys sintered in argon. This may be due to the formation of the second phase solid solution, more slow than that of Al_2OC alone, in the same way as the reduced densification rate of SiC–Al_2OC in N_2 compared to Ar has been attributed[5] to the formation of aluminium oxynitride by partial nitridation of Al_2O_3.

Optical microscopy on the pressureless sintered material revealed a significant amount of fine porosity ($< 20\,\mu m$ in size) and a regular distribution of the second phase throughout the material. Examination by transmission electron microscopy shows that both phases of the composite have equiaxed grain structures, and the triple junction grain boundaries seem free of glassy phase, especially taking into account the angular shapes of the crystal edges (Fig. 5). The majority of the SiC grains are in the range 1–4 μm, with the maximum grain size around 4 μm.

The mechanical properties of some SiC–2AlN.Al_2OC composites are listed in Table 3, as well as those of similar materials. It is seen that the Young's modulus and hardness of hot-pressed materials with 95 and 90 wt% SiC are close to those mentioned in the literature for pure SiC, and that their creep rates at 1400 and 1500 °C are improved. Not reported in the table is the (SEVNB) fracture toughness of the hot-pressed composites with 90 wt% SiC, namely 4·2 MPa.m.$^{1/2}$

Fig. 5. TEM micrograph of hot-pressed composite with 90 wt% SiC.

Table 3. Structural properties of some SiC–2AlN·Al2OC composites and similar materials

Material	H_v *(GPa)*	σ_f *(MPa)*	$\dot{\varepsilon}$ *(s^{-1})* at 1400 °C	$\dot{\varepsilon}$ *(s^{-1})* at 1500 °C	*E (GPa)*
These composites					
95 wt% SiC, HP	27·80	670 ± 170	$9{\cdot}7\times10^{-9}$	$5{\cdot}5\times10^{-8}$	420
90 wt% SiC, HP	27·10	620 ± 170	$1{\cdot}4\times10^{-8}$	$3{\cdot}8\times10^{-8}$	410
80 wt% SiC, HP	22·40	580 ± 130	n.d.	n.d.	n.d.
70 wt% SiC, HP	21·90	600 ± 110	n.d.	n.d.	n.d.
90 wt% SiC, PS	27	500 ± 60	n.d.	n.d.	360
SiC, HP (B,C additives)	28·4$^{(22)}$	n.a.	$2\times10^{-8(23)}$	$7\times10^{-8(23)}$	437$^{(22)}$
SiC–Al_2OC alloys					
90 wt% SiC, HP$^{(5)}$	23	650 ± 30	n.a.	n.a.	360
90 wt% SiC, PS$^{(5)}$	n.a.	310 ± 25	n.a.	n.a.	n.a.

HP: hot-pressed; PS: pressureless sintered; n.d.: not determined; n.a.: not available.

for comparison, similar measurements performed on commercial, pressureless sintered SiC materials reached values in the range 2·8–3·1 MPa.m.$^{1/2}$ It also appears that for the hot-pressed composite with 90 wt%SiC, the creep is less thermally activated, which could make it a useful structural ceramic at even higher temperatures. The decrease in Young's modulus observed with the pressureless sintered material containing 90 wt% SiC, compared to its hot-pressed counterpart, reflects the increased porosity. The flexural strength of both composites is comparable with the four point bend strength of hot-pressed materials with 10 wt% Al_2O_C,[5] but their hardness and Young's modulus are larger. Also larger, is the bend strength of pressureless sintered materials with 10 wt% 2AlN.Al_2OC, compared to the material with 10 wt% Al_2OC. Eventually, for the composite with 10 wt% 2AlN.Al_2OC, it is seen on Fig. 6 that its Young's modulus is retained up to 1300 °C and slightly weakens above that temperature, although the stress-strain curve at 1500 °C remained perfectly linear up to 300 MPa. As for the modulus of rupture (Fig. 7), it retains high values up to 1400 °C before slightly decreasing, thus demonstrating the highly refractory nature of the 2AlN.Al_2OC second phase and the strong cohesion between both phases of the composite.

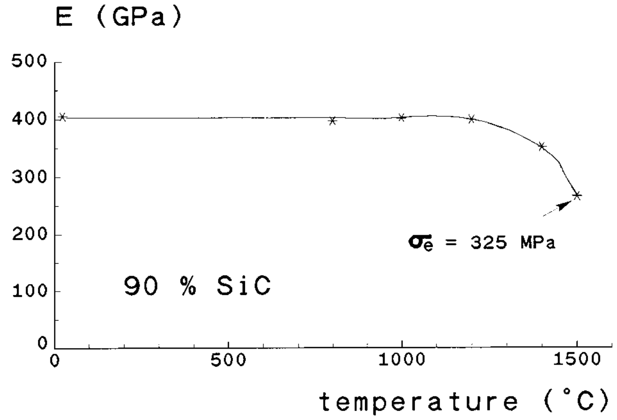

Fig. 6. Young's modulus of 90 wt% SiC composite between room temperature and 1500 °C.

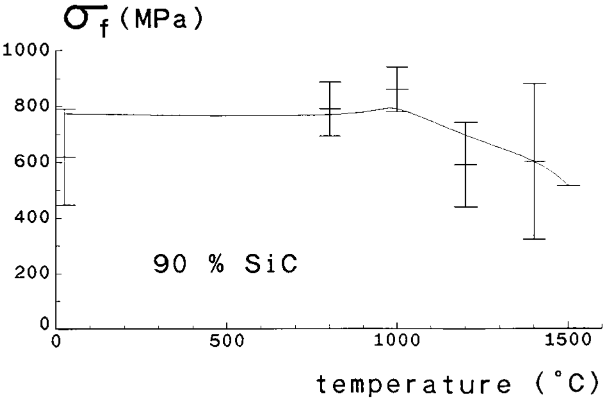

Fig. 7. Modulus of rupture of 90 wt% SiC composite between room temperature and 1500 °C.

4 Summary and conclusions

Standard Gibbs free energies of formation of aluminium oxycarbides Al_4O_4C and Al_2OC are given, and the stability diagram of the Al–C–O system is shown at 2100 K.

SiC-based composites are described, where the second phase is the würtzite compound 2AlN. Al_2OC. The properties of the composites with 5 and 10 wt% second phase are close to those of SiC and slightly higher than those of SiC–Al_2OC alloys. The existence of a miscibility gap near 2000 °C, between an SiC-rich phase and a (2H)-rich phase, is shown. Future work should assess the evolution of structural properties after long time exposures to high temperatures.

Acknowledgements

The authors are grateful to Dr C. Qiu for useful discussions and to the companies 'Céramiques et Composites' (F), 'ESK' (G) and 'Saint-Gobain-Norton Industrial Ceramics' (USA), for their interest in these materials and for providing standard samples of pressureless sintered silicon carbide.

References

1. Prochazka, S., Sintering of silicon carbide. In *Ceramics for High Performance Applications*, ed. A. E. Goram, J.J. Burke and R.N. Katz. Brook Hill Publ. Co., Chestnut Hill, MA, 1975, pp. 239–252.
2. Coppola, J.A., Hailey, L.N. and McMurtry, C.N., Process for producing sintering silicon carbide ceramic body. U.S. Patent 4124667, Nov. 7, 1978.
3. Omori, M. and Takei, H., Pressureless sintering of SiC. *J. Am. Ceram. Soc.*, 1982, **65**, C-92; Composite silicon carbide sintered shapes and its manufacturing. U.S. Patent 4502983, March 5, 1895; Method for preparing sintered shapes of silicon carbide. U.S. Patent 4564 490, Jan. 14, 1986.
4. Huang, J. L., Hurford, A. C., Cutler, R. A. and Virkar, A. V., Sintering behavior and properties of SiCAlON ceramics. *J. Mat. Sci.*, 1986, **21**, 1448–1456.
5. Jackson, T. B., Hurford, A. C., Bruner, S. L. and Cutler, R. A., SiC-based ceramics with improved strength. In *Proceedings of the Conference on Silicon Carbide (1987)*, ed. J.E. Cawley and C. Semler. American Ceramic Society, Colombus, OH, 1970, pp. 227–240.
6. Lihrmann, J. M., Zambetakis, T. and Daire, M., High temperature behavior of the aluminum oxycarbide Al_2OC in the system Al_2O_3–Al_4C_3 and with additions of aluminum nitride. *J. Am. Ceram. Soc.*, 1989, **72**(9), 1704–1709.
7. Lihrmann, J. M., Importance of the liquid phase for the processing of structural ceramics in the SiCAlON system. In *Structual Ceramics: Processing, Microstructure and Properties*, ed. J. B. Bentzen, J. J. Bilde-Sorensen and N. Christiansen. Riso National Laboratory, Roskilde, Denmark, 1990, pp. 395–402.
8. Qiu, C. and Metselaar, R., Thermodynamic evaluation of the Al_2O_3–Al_4C_3 system and stability of Al-oxycarbides. *Z. Metallk.*, 1995, **86**, 198–205.
9. Qiu, C. and Metselaar, R., Phase relations in the aluminum carbide-aluminum nitride-aluminum oxide system. *J. Am. Ceram. Soc.*, 1997, **80**(8), 2013–2020.
10. Awaji, H. and Sakaida, Y., V-notch technique for single-edge notched beam and chevron notch methods. *J. Am. Ceram. Soc.*, 1990, **73**(11), 3522–3523.
11. Munz, D., Bubsey, R. T. and Shanon, J. L., Fracture toughness determination of Al_2O_3 using four-point bend specimens with straight-through and chevron notches. *J. Am. Ceram. Soc.*, 1980, **63**(5–6), 300–305.
12. Fett, T. and Munz, D., *Mechanical Testing of Engineering Ceramics at High Temperatures*. Elsevier Applied Science, Oxford, 1989.
13. Yokokawa, H., Fujishige, M., Ujie, S. and Dokiya, M., Phase relations associated with the aluminum blast furnace: aluminum oxycarbide melts and Al–C–X (X=Fe, Si) liquid alloys. *Metall. Trans. B*, 1987, **18B**, 433–444.
14. Kuo, S.Y and Virkar, A. V., Phase equilibria and phase transformation in the AlN–Al_2OC pseudobinary system. *J. Am. Ceram. Soc.*, 1989, **72**(4), 540–550.
15. JANAF, *Thermochemical Tables*, 2nd edn. National Bureau of Standards, 1971.
16. Lihrmann, J. -M., SiCAlON ceramics. In *Advanced Materials*, ed. R. J. Brook, D. Bloor, S. Mahajan and M. C. Flemings. Pergamon Press, Oxford, 1994, pp. 2451–2454.
17. Zangvil, A. and Ruh, R., Phase relationships in the SiC–AlN system. *J. Am. Ceram. Soc.*, 1988, **71**(10), 884–990.
18. Kranzmann, A., Aluminum nitride. In *Advanced Ceramic Materials*, ed. R. J. Brook. Pergamon Press, Oxford, 1991, pp. 8–9.
19. Schwetz, K. private communication (1997).
20. Riley, F., Silicon carbide. In *Advanced Ceramic Materials*, ed. R. J. Brook. Pergamon Press, Oxford, 1991, pp. 426–429.
21. Lihrmann, J.-M. and Tirlocq, J., Procédé de préparation de produits céramiques densifiés et produits céramiques ainsi obtenus. French Patent 2737489, 2 Jul 1997; Process for producing dense products based on silicon carbide, and composite products thus obtained. European Patent Appl. WO9706119, 20 Feburary 1997.
22. Kim, S. and Kriven, W. M., Preparation, microstructure, and mechanical properties of SiC–Dy_2O_3 composites. *J. Am. Ceram. Soc.*, 1997, **80**(12), 2997–3008.
23. Nose, T., Fuji, T. and Kubo, H., In *Proc. MRS Int. Meeting on Advanced Materials*, ed. Materials Research Society, 1988, p. 293.
24. Zaretskaya, G. M., Eidel'shtein, F. I. and Sokhor, M. I., Aluminum oxycarbide in oxysulfide slag. Translated from. *Akad. Nauk SSSR, Neorg. Mat.*, 1972, **8**(1), 84–87.